



# The interaction of first- and second-order cues to orientation

S.C. Dakin \*, C.B. Williams, R.F. Hess

*McGill Vision Research, Department of Ophthalmology, 687 Pine Avenue West, Montreal, Quebec H3A 1A1, Canada*

Received 15 July 1998; received in revised form 9 November 1998

---

## Abstract

The visual system is sensitive to orientation information defined both by first-order (luminance) and by second-order (texture) cues. We consider how these orientation cues are computed and how they affect one another. We measured the perceived orientation of the first and second-order components of Gabor patches (the *carrier* and *envelope*, respectively) and report a dependence of the perceived orientation of each on the orientation of the other, and on the spatial frequency of the carrier. Fixing the carrier orientation near that of the envelope interferes with envelope orientation judgements. This interference is reduced by adding a small (subthreshold) rotation to the carrier indicating that the site of interference is early. When the gross relative orientation of carrier and envelope is varied, the carrier appears systematically tilted *towards* the envelope. However, provided envelope and carrier are separated by more than approximately 10°, the perceived envelope orientation appears tilted *away* from the carrier. The size of these effects increases with decreasing carrier spatial frequency, and with increasing exposure duration. When the envelope and carrier are both non parallel and non-perpendicular Fourier energy is distributed asymmetrically across orientation. We demonstrate that, for a channel-based orientation code, this asymmetry induces a shift in mean orientation that is sufficient to explain illusory tilting of carriers. The illusory tilting of the envelope, as a function of carrier orientation and spatial frequency, demonstrates that human ability to demodulate contrast information is far from ideal and cannot be explained by existing two-stage filter-rectify-filter models. We propose that illusory tilting of the envelope is due to selective connectivity between first- and second-stage filters whose purpose is to *dissociate* the type of image structure producing each class of cue. © 1999 Elsevier Science Ltd. All rights reserved.

*Keywords:* Orientation; Second-order; Texture; Contour

---

## 1. Introduction

Human detection of structure in images is not limited by the operation of linear, visual filters. There is accumulating psychophysical and neurophysiological evidence for sensitivity to second-order visual structure in a variety of perceptual domains, such as form (Henning, Hertz & Broadbent, 1975), motion (Chubb & Sperling, 1988), stereo (Hess & Wilcox, 1994), etc. The prevalent interpretation of these results is in terms of two classes of two-stream models (Henning et al., 1975; Chubb & Sperling, 1988; Wilson, Ferrera & Yo, 1992; but see also Johnston, McOwan & Buxton, 1992). The first class, early non-linearity or hybrid models, employ

a single filtering stage with input coming either directly from the stimulus or from the result of applying an early non-linearity to the stimulus (Henning et al., 1975). Such schemes, relying as they do on distortion products, predict that second-order structure such as contrast modulation should behave exactly as first-order structure (luminance modulation). A variety of data have shown that this is not the case. For example it has been demonstrated psychophysically, that sensitivity to beats is highest when the grating components forming the beat have the same amplitude (Derrington & Badcock, 1986). A model using an early non-linearity to detect second-order structure predicts that sensitivity should depend on the *product* of the component amplitudes. Additionally, the motion of a drifting contrast modulation is not nulled by the addition of a luminance grating which nulls the distortion product (Badcock & Derrington, 1989). Finally, cells in area 18 of feline visual cortex respond to second-order motion and are

---

\* Corresponding author. Present address: Department of Visual Science, Institute of Ophthalmology, 11-43 Bath Street, London EC1V 9EL, UK.

*E-mail address:* s.dakin@ucl.ac.uk (S.C. Dakin)

tuned for both the spatial frequency (Zhou & Baker, 1993, 1994, 1996) and orientation (Mareschal & Baker, 1998) of the carrier and envelope components of moving second-order stimuli. Reliance on the output of an early non-linearity would predict similar tuning for both envelope and carrier.

### 1.1. Filter-rectify-filter models

To address these weaknesses a two-stream filter-rectify-filter (FRF) model has been proposed (Chubb & Sperling, 1988; Wilson et al., 1992). The FRF model has a first stream composed of a linear spatio-temporal filter bank. The second stream receives input from the first, applies a severe non-linearity (usually full- or half-wave rectification; Chubb & Sperling, 1988) and then convolves the result with a bank of filters tuned to proportionally lower spatio-temporal frequencies than the preceding filter bank. Such an approach has been used to account for a variety of second-order motion (Wilson et al., 1992; Zhou & Baker, 1993; Wilson & Kim, 1994; Lu & Sperling, 1995) and texture (Malik & Perona, 1990; Graham, Beck & Sutter, 1992) phenomena.

Notice that the model shown in Fig. 1 has complete connectivity between different orientations of first- and second-stage filters. A basic prediction of such a scheme is that psychophysical tasks requiring demodulation of a second-order cue will show no dependency on the first-order structure in the image. This paper tests that prediction.

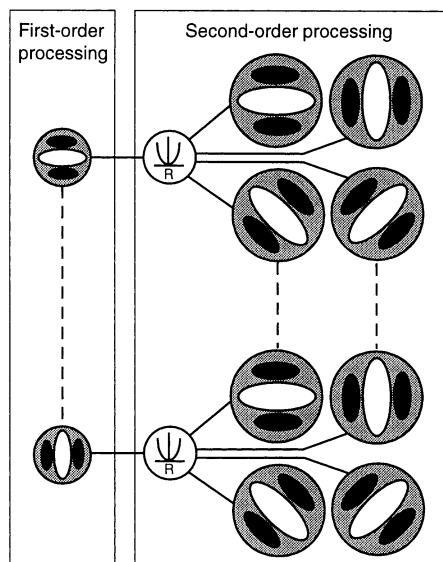


Fig. 1. The filter-rectify-filter two-stream model. The output from all first- and second-stage processes is independently available and we refer to this as the fully connected FRF scheme.

### 1.2. The independence of first- and second-order cues to orientation

There is little direct psychophysical work directly examining the independence of first- and second-order cues to orientation. Indeed, the use of amplitude modulated isotropic band-pass noise (e.g. Sutter, Sperling & Chubb, 1995), has set out to explicitly avoid such interactions. There is evidence from the second-order motion literature that the notional first- and second-order filters are not independent. Cropper and Badcock (1995) have reported that the perceived direction of an amplitude-modulated plaid is strongly dependent on the orientation bandwidth of the carrier. This finding suggests that, contrary to the prediction of an FRF model, the extraction of a second-order motion signal is strongly dependent on the orientation structure of the carrier.

Lin and Wilson (1996) used D6 contrast-modulated cosine gratings and report an interaction between the orientation of the carrier grating and the vertical contrast envelope. Orientation discriminability thresholds for the modulation rose by a factor of 1.4 when the cosine grating was oblique compared to when it was horizontal. This is an intriguing result as the model shown in Fig. 1 would predict no such interaction.

Dakin and Mareschal (submitted) measured sensitivity to contrast modulation of band-pass noise carriers. For isotropic carriers, thresholds show an inverse dependence on the spatial frequency of the carrier. For oriented carriers at low spatial-frequencies, thresholds for detecting contrast modulation vary in inverse proportion to the difference in orientation between the carrier and envelope, performance being very poor when carrier and envelope are at the same orientation. This dependence on carrier orientation diminishes as the spatial frequency of oriented carriers is increased. Detection of contrast modulated oriented noise, in the presence of unmodulated noise masks, indicates that the contrast demodulation system receives input from oriented filters.

McOwan and Johnson (1995) report that the perceived orientation of the envelope component of a contrast modulated grating depends on the carrier orientation. Fig. 2(a) shows typical stimuli of the sort they used: an oblique sine-wave carrier modulated by a vertical contrast envelope. Notice that the perceived orientation of both the low-contrast regions and the barber-poles, appear tilted towards the carrier orientation. McOwan and Johnson (1995) use this illusion, and its space-time analogue, to demonstrate a difference in the visual representation of orientation in space-space and space-time but do not consider the implications of the interference between carrier and envelope for existing models of second-order processing.

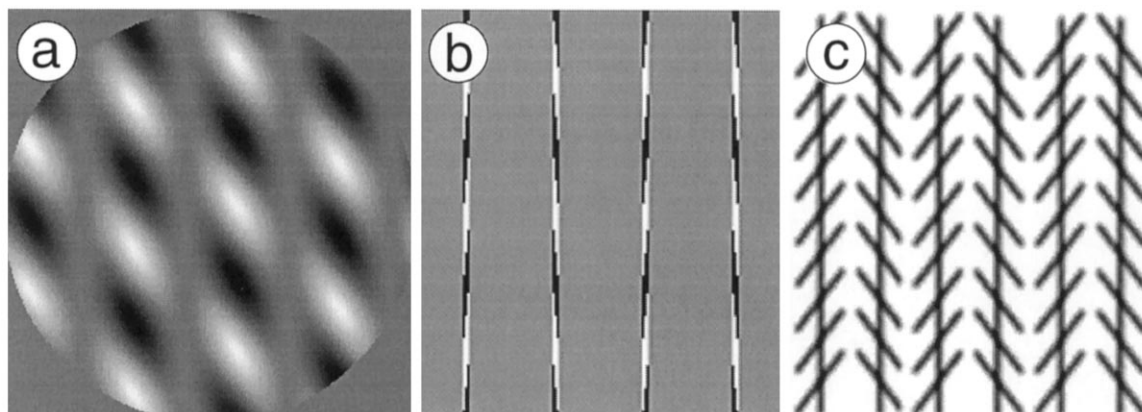


Fig. 2. (a) A sine wave grating modulated by a vertical contrast envelope. (b) Fraser cords and (c) the Zöllner illusion. For (b) and (c), carrier orientation is traditionally mirror-reversed between alternate segments to enhance the illusion.

The illusion induced by Fig. 2(a) is clearly related to the well-known Münsterberg or Fraser illusions (e.g. Münsterberg, 1897), a variant on which (Fraser cords; Morgan & Moulden, 1986), is shown in Fig. 2(b). Again, notice the perceived tilting of the barber-poles towards the carrier/stripe orientation. An intriguing aspect of the Fraser is that the perceived tilt is in the opposite direction to that produced by the Zöllner illusion (Fig. 2(c); Zöllner, 1862). The vertical lines of the Zöllner appear tilted away from the intersecting obliques, but Fraser verticals tilt towards the stripes. Such illusions are considered to be the result of the orientation of local components interfering with global orientation. Similarities between Fig. 2(a) and Fig. 2(b, c) suggest that, for these illusions, global orientation may be equivalent to second-order orientation, and that the study of interactions between first- and second-order cues to orientation could offer insights into illusions which remain unexplained more than a century after their discovery.

We set out to investigate interactions between first- and second-order cues using Gabor patches, which are composed of a sinusoidal carrier grating windowed by an oriented Gaussian envelope. By varying the relative orientation of the envelope and carrier component one can control the degree of discrepancy between first- and second-order orientation components of the stimulus.

## 2. General methods

### 2.1. Subjects

Two of the authors and one naïve subject served as observers in all experiments. SCD and CD are corrected-to-normal myopes, and SCD has a small (0.25 D) corrected astigmatism. Observers underwent a short training period prior to threshold measurement.

### 2.2. Apparatus

Stimuli were generated and presented using a Macintosh 7500 microcomputer which also recorded subjects' responses. Stimuli were displayed on a Nanao Flexscan 6500 monochrome monitor, with a frame refresh rate of 75 Hz. Luminance levels were linearised using a look-up table derived using programs from Denis Pelli's VideoToolbox package (Pelli, 1997), from which display routines were also derived. The screen was viewed binocularly at a distance of 243 cm and had a mean background luminance of 47.5 cd/m<sup>2</sup>.

### 2.3. Stimuli

Stimuli were composed of patches with luminance modulated by sinusoidal gratings multiplied by a two-dimensional Gaussian envelope (Gabor patches). This function has the form:

$$G(x) = L_0 + L_0 C \sin(2\pi\omega x_c + \phi) \exp\left[-\frac{x_e^2}{\sigma_x^2} - \frac{y_e^2}{\sigma_y^2}\right] \quad (1)$$

where  $L_0$  is the mean luminance and  $C$  the contrast,  $\sigma_x$  and  $\sigma_y$  are the standard deviations of the Gaussian envelope in the  $x$ - and  $y$ -directions, and  $\omega$  and  $\phi$  are the spatial frequency and phase, respectively, of the modulating sinusoid. All stimuli were luminance balanced ( $\phi$  set to 0°).  $x_e$  and  $y_e$  are co-ordinates rotated by the envelope angle  $\theta_e$ :

$$\begin{aligned} x_e &= x \cos \theta_e + y \sin \theta_e \\ y_e &= y \cos \theta_e - x \sin \theta_e \end{aligned} \quad (2)$$

and  $x_c$  is the  $x$ -coordinate rotated by the carrier angle  $\theta_c$ :

$$x_c = x \cos \theta_c + y \sin \theta_c \quad (3)$$

(Throughout this paper  $0^\circ$  denotes horizontal and  $90^\circ$  denotes vertical. Thus a negative angular offset indicates clockwise rotation, and a positive angular offset indicates anti-clockwise rotation).

Patches were generated on-line and were spatially truncated at  $\pm 5\sigma_x$  ( $\sigma_x$  was always the larger of the two parameters defining the envelope and was fixed at  $0.5^\circ$ ). Unless stated otherwise, patches had contrast fixed at 0.84, the aspect ratio of the envelope was 3:1 (i.e.  $\sigma_y = 0.17^\circ$ ), and the spatial frequency of the modulating sinusoid was 4 cpd. The independent variable in all conditions was an offset added to the orientation of either the carrier or the envelope component of the Gabor. Stimuli were presented for 100 ms. and were positioned randomly in a 32 pixel radius region around the centre of the display.

#### 2.4. Procedure

In each experiment a single-interval, two alternative forced choice (2AFC) procedure was used. Subjects were presented with a Gabor micro-pattern and were required to make a judgement about either the carrier or envelope component, depending on the condition. That is subjects indicated whether the component of interest was clockwise or anti-clockwise of an internal vertical standard. A method of constant stimuli was used to sample the psychometric function. Each block consisted of 288 trials. This consisted of 16 presentations at 17 stimulus levels. In the first run stimulus levels corresponded to orientation offsets of  $-8^\circ$  to  $+8^\circ$ , inclusively. The psychometric function was derived by performing a least-squares-fit of a cumulative Gaussian to the raw data. The cumulative Gaussian is defined as:

$$p(x) = 0.5 \operatorname{erf}\left(\frac{x - \mu}{\sqrt{2}\sigma}\right) + 0.5 \quad (4)$$

where  $\sigma$  is the threshold; the slope of the function. This corresponds to the precision of the judgement (the stimulus level producing 84% correct performance). The offset parameter  $\mu$ , is a measure of the bias or accuracy (the stimulus level producing 50% correct performance).

Having established the approximate point of subjective verticality (i.e. the parameter  $\mu$ ) the stimulus range presented was set to  $-(8 + \mu)^\circ$  to  $+(8 + \mu)^\circ$ , inclusively. This ensures subjects were responding clock-wise or anti-clockwise an approximately equal number of times within a run.

### 3. Experiment 1: subthreshold interaction of first- and second-order orientation

The first experiment used a paradigm akin to subthreshold summation (Graham, 1989) to examine the

question of how interwoven first- and second-order orientation computations are. This technique involves the comparison of thresholds measured for compound stimuli, composed of two cues, to thresholds for simple stimuli containing only one of the two cues. If the two cues are not processed independently then thresholds for the compound stimuli may be lower than for the simple stimuli. This technique has been widely used to study the bandwidth of mechanisms underlying visual detection (Graham & Nachmias, 1971) and location (Kulikowski & King-Smith, 1973; Wilson, 1978). In this case we measured discrimination thresholds for first- and second-order cues to orientation. Note that while a subthreshold summation paradigm typically assumes that summation occurs within a single channel, we are making a rather different assumption. We suggest that if separate (probably channel-based) representations of first- and second-order orientation information exist it is possible that they interact before the output of either reaches detection threshold. This experiment tests that hypothesis.

#### 3.1. Method

Gabor stimuli were generated with peak spatial frequency of 4 cycles per degree and a contrast ( $C$ ) of 0.09. We used relatively low-contrast stimuli in order to elevate the baseline threshold for envelope orientation discrimination which we reasoned might make small facilitatory effects more apparent. We first estimated orientation discrimination thresholds for the carrier. This involved subjects making a single interval judgement of the orientation (clockwise versus anti-clockwise of vertical) of the carrier component of a Gabor with a fixed vertical envelope. Carrier orientations were sampled using the method of constant stimuli described above, and data were fit with a cumulative Gaussian to give an estimated threshold of  $0.75^\circ$  for both subjects. In the main experimental condition which followed the independent variable was the orientation of the patch envelope. Other experimental details were similar to the carrier orientation judgement (i.e. single interval judgement around vertical, method of constant stimuli, etc.) However in this condition, the carrier component also had a subthreshold cue ( $0.0$ – $0.6^\circ$ ) added, in the direction of the envelope cue, to the baseline carrier orientation of  $90^\circ$ . In a control condition we measured envelope orientation discrimination thresholds with a carrier fixed at  $0^\circ$  (horizontal). Examples of the stimuli (presented at maximum contrast) are shown in Fig. 3.

#### 3.2. Results

Results for two subjects are shown in Fig. 4. While absolute thresholds are variable across the two observers, adding a subthreshold cue to the carrier orientation

clearly improves performance compared with when the carrier is fixed at vertical. This indicates that the site of interaction between these two sources of information must be early. However notice that as the size of the carrier cue increases, discrimination of envelope orientation does not exceed performance for stimuli with a horizontal carrier (upper dashed line). The carrier orientation of this stimulus contributes nothing to the envelope. It appears that tilting the carrier in the direction of the envelope cue does not lead to combination of information but instead to a reduction in a source of interference for envelope discrimination. The FRF scheme as described predicts no such interaction.

#### 4. Experiment 2: effect of relative orientation of carrier and envelope on judgements of their orientation

The previous experiment reported that fixing the carrier at orientations within a few degrees of the envelope interferes with judgement of the envelope orientation. In this experiment we extended this finding by examining the effect of gross differences between carrier and envelope orientation on judgements of each component's orientations.

Changing the second-order structure of a Gabor patch also alters the first-order orientation information; for example, the bandwidth of a fixed carrier depends

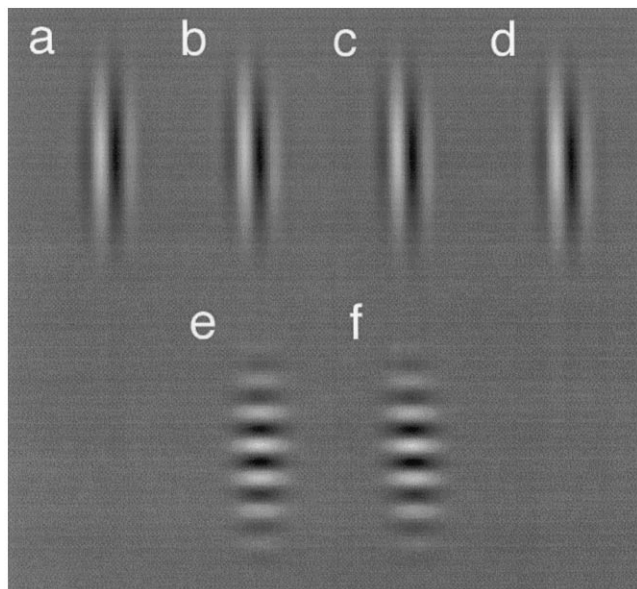


Fig. 3. Gabor patches used in Experiment 1. (a, b) Shows patches with fixed vertical carriers, windowed by envelopes of 90 and 92.5° (i.e. 2.5° anti-clockwise of vertical), respectively. The tilt of the envelope is difficult to detect. (c, d) Show stimuli with 92.5° envelopes and a (c) 0.2° and (d) 0.4° cue added to the carrier. Detection of envelope tilt in (d) is more apparent than (b). (e, f) Illustrate the control condition; a horizontal carrier windowed by envelopes of (e) 90° and (f) 92.5°.

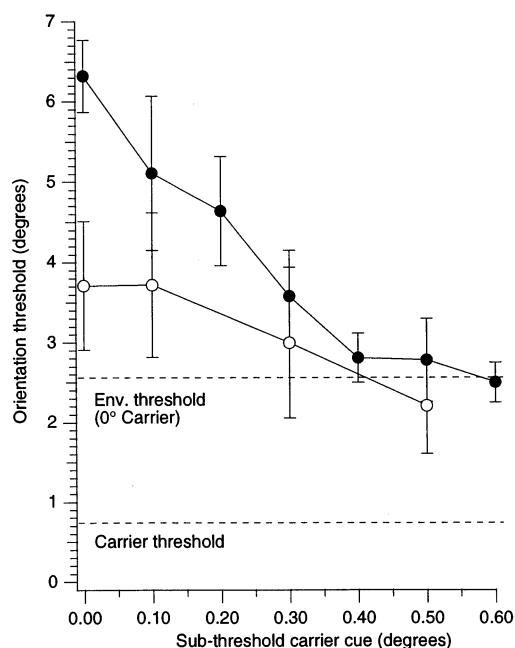


Fig. 4. Orientation discrimination of the envelope component of a Gabor as a function of a subthreshold orientation cue added to the carrier. Notice that cueing the carrier improves envelope discrimination but not beyond performance for an envelope with a fixed 0° carrier. (Filled symbols, SCD; open symbols, CBW; error bars show  $\pm 1$  standard error).

solely on envelope orientation<sup>1</sup>. The first purpose of this experiment was to quantify the influence of second-order structure on perceived first-order structure and to evaluate if the magnitude of this influence extends beyond what would be expected from the change to the first-order structure alone (indicating purposeful early combination of first- and second-order cues). By contrast, altering the first-order component of a Gabor patch in no way alters its second-order structure. If the visual system efficiently demodulates the envelope (in the manner suggested by a fully connected filter-rectify-filter scheme) one would expect no influence of carrier on perceived envelope orientation. The second purpose of the experiment was to investigate if observers are capable of efficient demodulation of the envelope component of Gabor stimuli, irrespective of carrier orientation.

Tyler and Nakayama (1984) used Zöllner stimuli (e.g. Fig. 1(c)) to examine the influence of local on global orientation structure. Their stimuli were composed of lines (analogous to our carrier) organised into global barber-poles (analogous to our envelopes). Because of this, their stimuli presented both first- and second-order cues to their global orientation. They found a complex pattern of interactions with carriers attracting envelopes when they were within approximately 10° of

<sup>1</sup> This point is expanded in Section 7 below.

one another, and otherwise repulsing perceived envelope orientation. Independently from this study, Morgan and Baldassi (1997) extended the Tyler and Nakayama (1984) study using Gabor stimuli with oriented envelopes, and showed a similar pattern of results which they relate to a collator unit model.

#### 4.1. Method

Stimuli were generated in the manner described in Section 2 (examples are shown in Fig. 5). All carriers had a peak spatial frequency of 4 cpd, envelopes had an aspect ratio of 3:1 ( $\sigma_x = 0.5^\circ$  and  $\sigma_y = 0.17^\circ$ ) and, unless stated otherwise, patches were presented at a contrast of 0.84. Orientation judgements were always made relative to an internal vertical standard, i.e. one component of the Gabor was always near-vertical. The effect of varying envelope and carriers was measured using orientations of  $0^\circ$  (horizontal), 15, 30, 45, 60, 75, 80, 85 and  $90^\circ$  (vertical). Pilot studies confirmed that the sign of orientation difference between carrier and envelope did not alter performance and so we only examined positive orientation differences (i.e. the near-vertical component, whose orientation was to be judged, was always anti-clockwise of the orientation of the other component).

We measured the proportion of stimuli categorised as clockwise as a function of the orientation of the cued

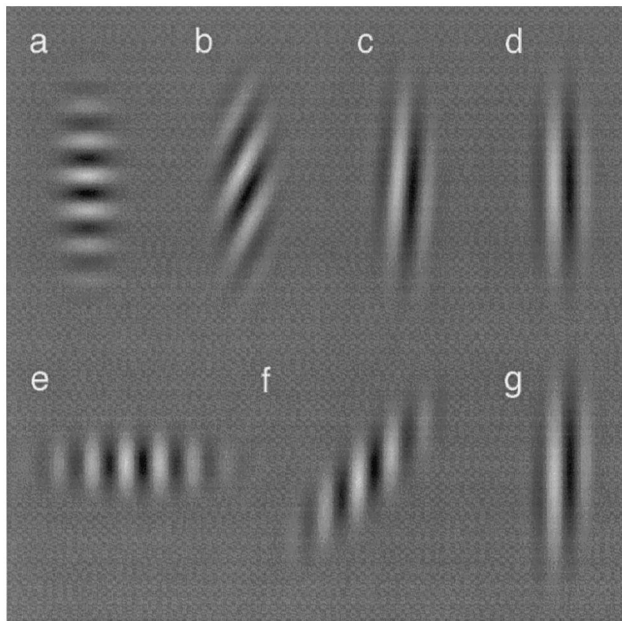


Fig. 5. Examples of the stimuli used in Experiment 2. (a–d) shows Gabors composed of a vertical ( $90^\circ$ ) envelope multiplied by a carrier of orientation (a)  $0^\circ$ ; (b)  $45^\circ$ ; (c)  $85^\circ$ ; and (d)  $90^\circ$ . Note the anti-clockwise and clockwise tilting of the envelope in (b) and (c), respectively. (e–g) shows Gabors composed of a vertical carrier multiplied by an envelope of (d)  $0^\circ$ ; (e)  $45^\circ$ ; and (e)  $85^\circ$ . Note the clockwise-tilting of the carrier in (f).

component of the pattern (either carrier or envelope). To each measured psychometric function we fit a cumulative Gaussian; the slope and offset of the fit give estimates of the subjects' precision/error and accuracy/bias.

#### 4.2. Results

Threshold and bias data from three subjects are shown in the left and right columns, respectively, of Fig. 6. Upper plots show carrier discrimination data, lower plots show envelope discrimination data. Fig. 6(a, c) illustrate that carrier and envelope orientation discrimination thresholds, for aligned carrier and envelope, are low<sup>2</sup> at around  $1.0^\circ$ . From the point where carrier and envelope are perpendicular ( $0^\circ$  on the abscissa in Fig. 6) thresholds rise steadily as the orientational difference between carrier and envelope decreases, peaking at a difference of  $45^\circ$  for carrier discrimination, but at nearer  $25\text{--}30^\circ$  for envelope discrimination. That near-vertical envelope orientation discrimination thresholds are higher with oblique than with horizontal carriers confirms the finding of Lin and Wilson (1996) (although we show a somewhat smaller effect—a factor of 1.2 deterioration compared to 1.4 as they reported). From the point of maximum error performance improves. In the case of envelope discrimination, thresholds approach  $1.5^\circ$  for parallel carrier and envelope. For carrier discrimination thresholds drop to around  $0.7^\circ$  which is actually lower than thresholds for perpendicular carrier and envelope. This is most likely attributable to the bandwidth of the stimulus being lower in the case of parallel, rather than perpendicular, carrier and envelopes. On the other hand, envelope discrimination performance is best when carrier and envelope are perpendicular. This is consistent with the results from the previous experiment; we conclude interference between the two sources can affect thresholds.

The right-hand set of plots in Fig. 6 illustrates that subjects show a systematic bias in their estimation of both envelope and carrier, the magnitude of which depends on the relative orientation of the two components of the Gabor. The most apparent feature of the data is the reversal in sign of the bias on carrier discrimination compared to performance with the envelope. Subjects systematically see the envelope component as tilted *away* from the carrier (lower plot), but the carrier as tilted *towards* the envelope (upper plot). The point of maximum illusory shift is around  $45^\circ$  for the

<sup>2</sup> In considering the threshold data from this condition we concentrate on the data from the experienced subjects. While the naive subject's performance show a broadly similar pattern we do not emphasise these data simply because they are based on fewer measurements.

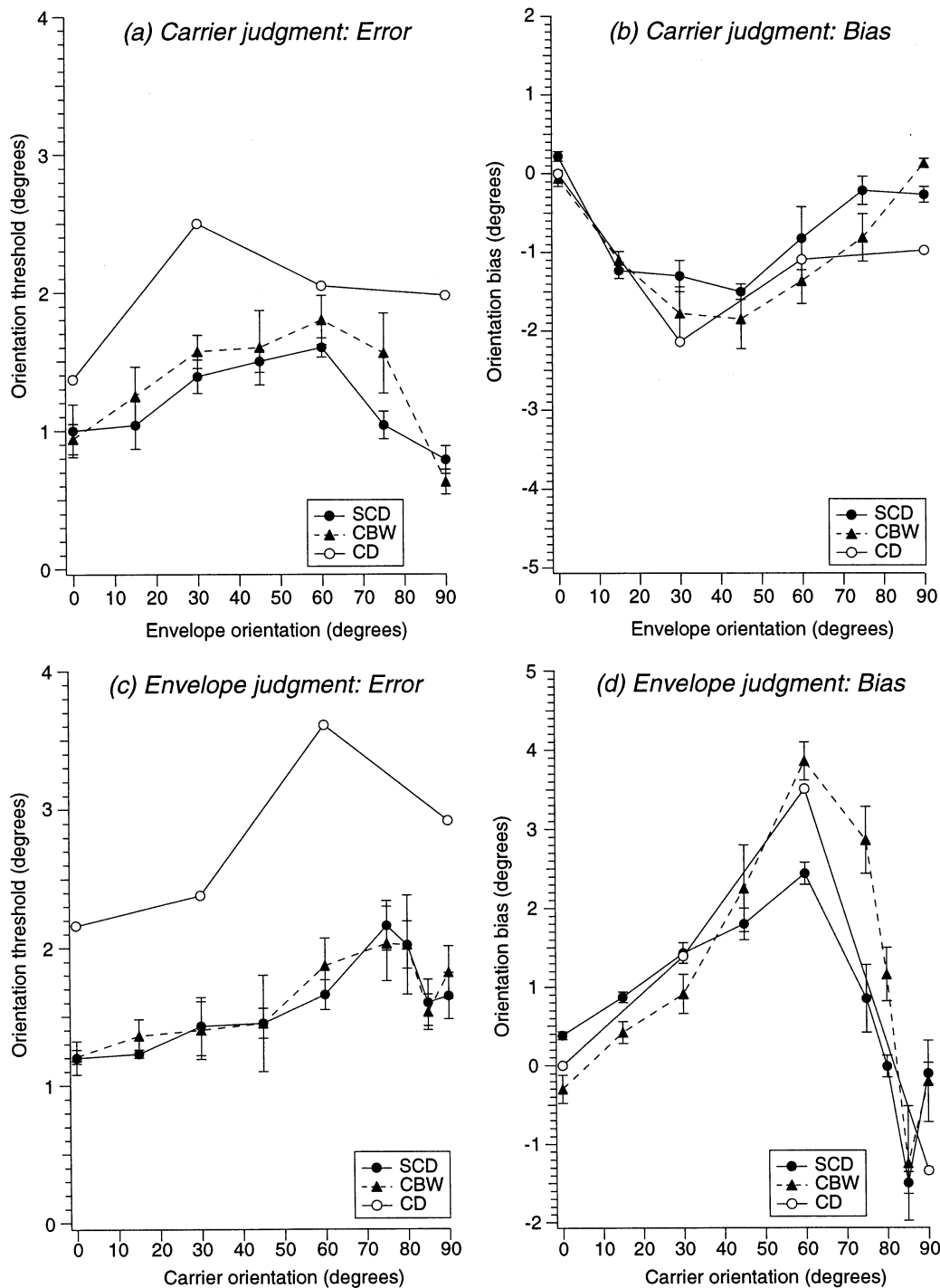


Fig. 6. Orientation discrimination performance of three observers for the carrier (a, b), and envelope (c, d) components of a Gabor micro-pattern. (a, c) shows thresholds, and (b, d) biases. The difference in the sign of biases shown in (b) and (d) indicate that subjects systematically saw the carrier orientation rotated towards the envelope, but the envelope orientation rotated away from the carrier.

carrier judgements, but nearer 60° for the envelope judgement. Notice also that the magnitude of the envelope illusion (mean 3.3°) is approximately twice that of the carrier (mean -1.7°).

The naïve subject's threshold data (open symbols in Fig. 6) indicate consistently more error-prone performance. Data are, however, in broad agreement with

trained subjects'. Interestingly, bias data from all subjects are in close agreement indicating that the magnitude of illusory orientation shifts are little affected by prolonged exposure to the stimuli. Both bias and threshold data for the envelope discrimination data are in close accord with data from other studies (Tyler & Nakayama, 1984; Morgan & Baldassi, 1997).

To summarise we have shown an interaction between envelope and carrier components of a Gabor pattern that leads to increased threshold and systematic biases on the estimation of the orientation of each component. In Section 7 we will show that the direction of perceived carrier tilt (towards envelope orientation) is consistent with the operation of a standard channel-based code for orientation. That the perceived envelope orientation should be repulsed by the carrier orientation is doubly intriguing. First, it argues against the independence of first- to second-order filter connectivity inherent in present FRF models. Second, it is inconsistent with the most obvious combination rule: a vector-sum (used to model combination of first- and second-order motion direction signals; Wilson et al., 1992) which would predict biases in the opposite direction. The effect is apparently not due to combination but interference. In the following experiment we examined the dependence of the effect on the spatial frequency and contrast of the carrier component.

### 5. Experiment 3: effect of carrier spatial frequency on judgements of carrier and envelope orientation

It has been proposed (e.g. Sutter et al., 1995) that first-stage filters are in a fixed spatial frequency relationship with the second-order mechanisms which they subserved. This experiment examined how both the precision and accuracy of orientation judgements depends on the spatial frequency relationship of carrier to envelope.

#### 5.1. Method

Stimuli were similar to those described above, except that spatial frequency of the carrier was systematically varied and the effect on envelope and carrier orientation discrimination was measured. All stimuli had a 45° orientation offset between carrier and envelope, i.e. the component to be judged was always near vertical, and the other was fixed at 45°. We chose this offset because it generated consistently large biases in carrier and envelope discrimination, as described in the last section. As a control we also performed several runs with the carrier and envelope fixed at both horizontal and vertical. These produced little or no interference across all conditions tested.

The carrier spatial frequency range tested was 2.0–22.3 cpd and examples of the stimuli are shown in Fig. 7. The range tested was bound both by subjects inability to reliably determine orientation with higher frequency carriers, and by the d.c. artifacts that are introduced when the carrier spatial frequency approaches that of the envelope. All carrier orientation judgements were made at a viewing distance of 243 cm.

However because we wished to determine if envelope discrimination was viewing distance dependent, we conducted these judgements at three viewing distances of 121, 243 and 486 cm.

#### 5.2. Results

Fig. 8 shows carrier orientation thresholds from three subjects. The U-shaped function (for two out of the three subjects) in Fig. 8(a) indicates that subjects are most accurate at judging the carrier orientation at a mid-range of spatial frequencies. Given that spatial frequency per se has little effect on accuracy at judging the orientation of supra-threshold grating in the spatial frequency range tested (e.g. Heeley & Buchanan-Smith, 1990; Burr & Wijesundra, 1991), this result is likely to be an interaction of carrier and envelope spatial frequency. The high thresholds observed at low carrier

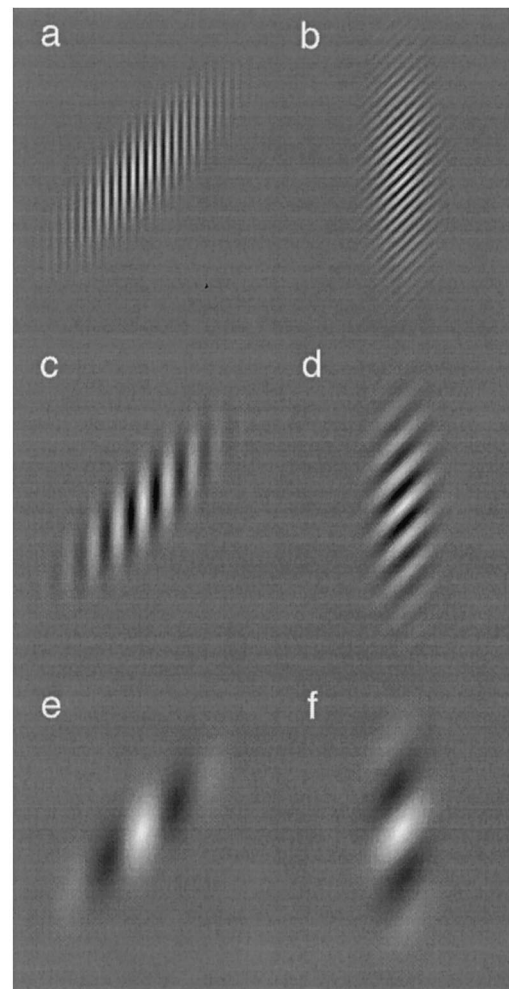


Fig. 7. Stimuli from Experiment 3. Under experimental viewing conditions, the carrier component of the Gabors has a peak spatial frequency of (a, b) 8.0 cpd; (c, d) 4.0 cpd; and (e, f) 2.0 cpd. Notice that the magnitude of the perceived tilt of both the carrier and the envelope increases with decreasing carrier spatial frequency.

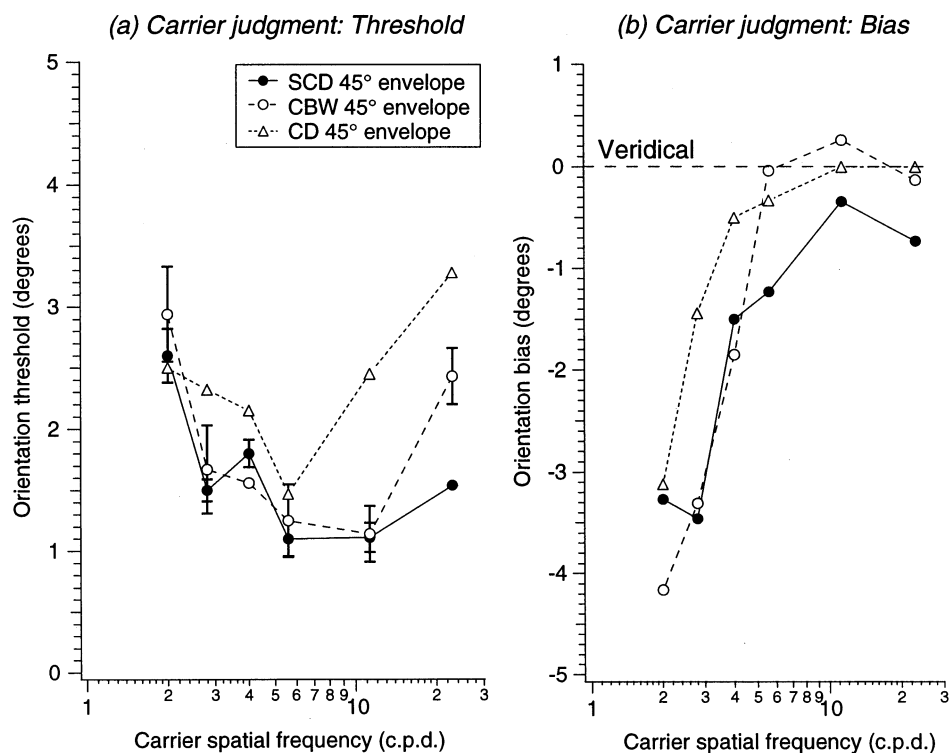


Fig. 8. The effect of carrier spatial frequency on carrier orientation judgements. (a) Accuracy is the highest at spatial frequencies falling in the mid range. (b) Subjects see the carrier as tilted towards the envelope orientation, and the size of this illusion is inversely proportional to carrier frequency.

spatial frequencies are likely to be attributable to the rise in carrier-bandwidth which occurs when the spatial frequency of a grating is decreased within a fixed size of envelope. Signals with a higher bandwidth stimulate a wider range of channels and consequently increase the subjects' uncertainty as to the true orientation. Performance improves with increasing spatial frequency (and decreasing bandwidth) but falls off at the highest frequencies tested (22.3 cpd for the experienced subjects) probably because of reduced visibility.

The bias data, shown in Fig. 8(b), indicate that subjects systematically see the carrier tilted towards the orientation of the envelope and the size of this illusory tilt varies in inverse proportion to the carrier spatial frequency. Notice that for high carrier frequencies ( $> 10$  cpd) these data illustrate a clear dissociation between threshold and bias; subjects are precise but inaccurate, and this pattern of bias is therefore unlikely to be due to uncertainty. Also notice that although the naïve subject's data are again more variable and error-prone, that her performance is broadly consistent with the authors'.

The effect of carrier spatial frequency on the envelope orientation was measured at three viewing distances, and data are graphed in Fig. 9. The first thing to notice is that subjects' data show similar trends, across the three viewing distances tested, when data

are plotted as a function of carrier spatial frequency in cycles per degree. If the task exhibited scale invariance we would expect curves to be shifted versions of one another, rank ordered by viewing distance, and separated by an octave on the abscissa. Generally data do not show this trend, even when curves do show some degree of separation (e.g. Fig. 9a). The finding that it is not cycles per envelope, but cycles per degree which determine subjects envelope discrimination performance is surprising. It means that the large envelope tilt induced by Fig. 7(f), for example, is reduced to the size of that induced by Fig. 7(d), by doubling the viewing distance, even though this leaves all carrier to envelope relationships unchanged. This again would seem to indicate that the sight of interference for this illusion is early.

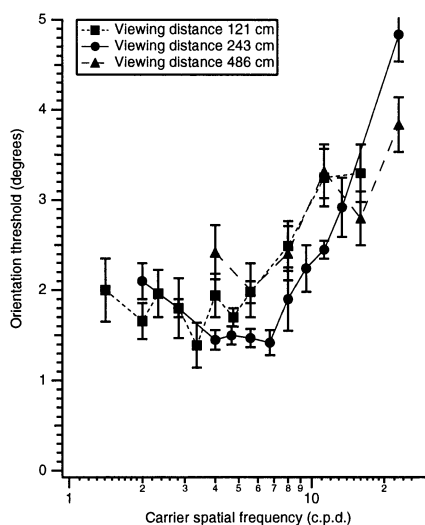
Thresholds from this condition (Fig. 9a, c) are quite different to those presented for the carrier judgement (Fig. 8a) which decreased with carrier spatial frequency (followed by a sharp increase at the very highest frequencies). Envelope thresholds show the reverse trend, and plateau at around 1.5–2.0° until carrier spatial frequencies reach around 8.0 cpd, beyond which performance deteriorates rapidly. Note that envelope discrimination drops off at carrier spatial frequencies much lower (1.5–2.0 octaves) than for carrier discrimination, and is therefore unlikely to be

attributable to a simple reduction in the visibility of the carrier component. Notice also that for a range of low carrier frequencies, subjects are more precise at judging the envelope than the carrier orientation which is attributable to the fact that envelope orientation bandwidth (unlike the carrier) is constant under changes to carrier spatial frequency. Bias data (Fig. 9b, d) show an inverse dependence on carrier spatial frequency. Although there is some indication of a notch around 5 cpd for both subjects at all viewing distances, the size of our sample does not allow us to determine if this is a reliable trend or simply a consequence of the greater variability of data in this condition.

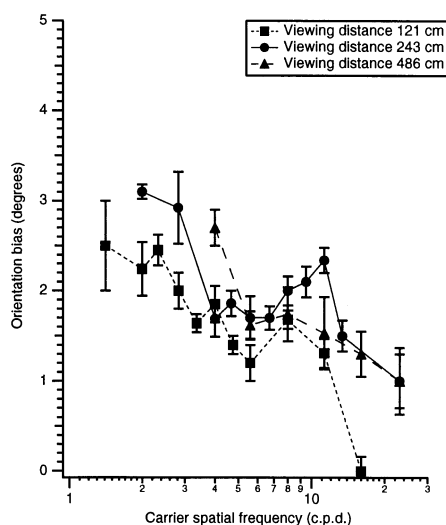
## 6. Experiment 4: effect of exposure duration on carrier and envelope orientation discrimination

Lin and Wilson (1996) compared the effect of exposure duration on judging the orientation of standard (first-order) D6 pattern with the same pattern modulating a cosinusoidal grating (second-order stimulus). They report no dependence of accuracy of first-order orientation judgements on exposure duration in the range tested (33.3–500 ms), but a loss in accuracy for second-order orientation judgements at the shortest exposure times. We sought to compare the accuracy and precision of judgements of first- and second-order components of our stimuli as a function of the exposure duration.

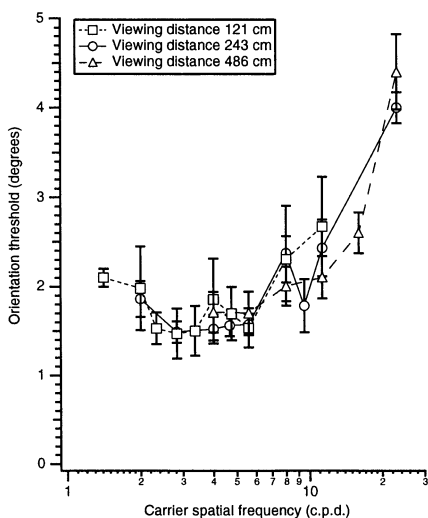
(a) Envelope judgment: Threshold,  $S=SCD$



(b) Envelope judgment: Bias,  $S=SCD$



(c) Envelope judgment: Threshold,  $S=CBW$



(d) Envelope judgment: Bias,  $S=CBW$

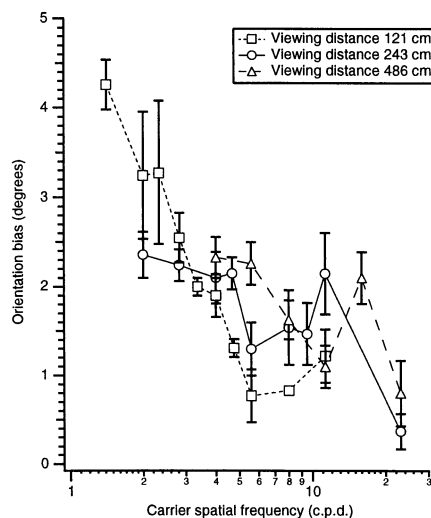


Fig. 9. Envelope discrimination as a function of carrier (c.p.d.) at three viewing distances. (a, c) thresholds and (b, d) biases, for two observers. Note the data are largely coincident when plotted as a function of carrier spatial frequency in cycles per degree. This indicates that neither the accuracy nor the precision of envelope orientation discrimination exhibits scale invariance.

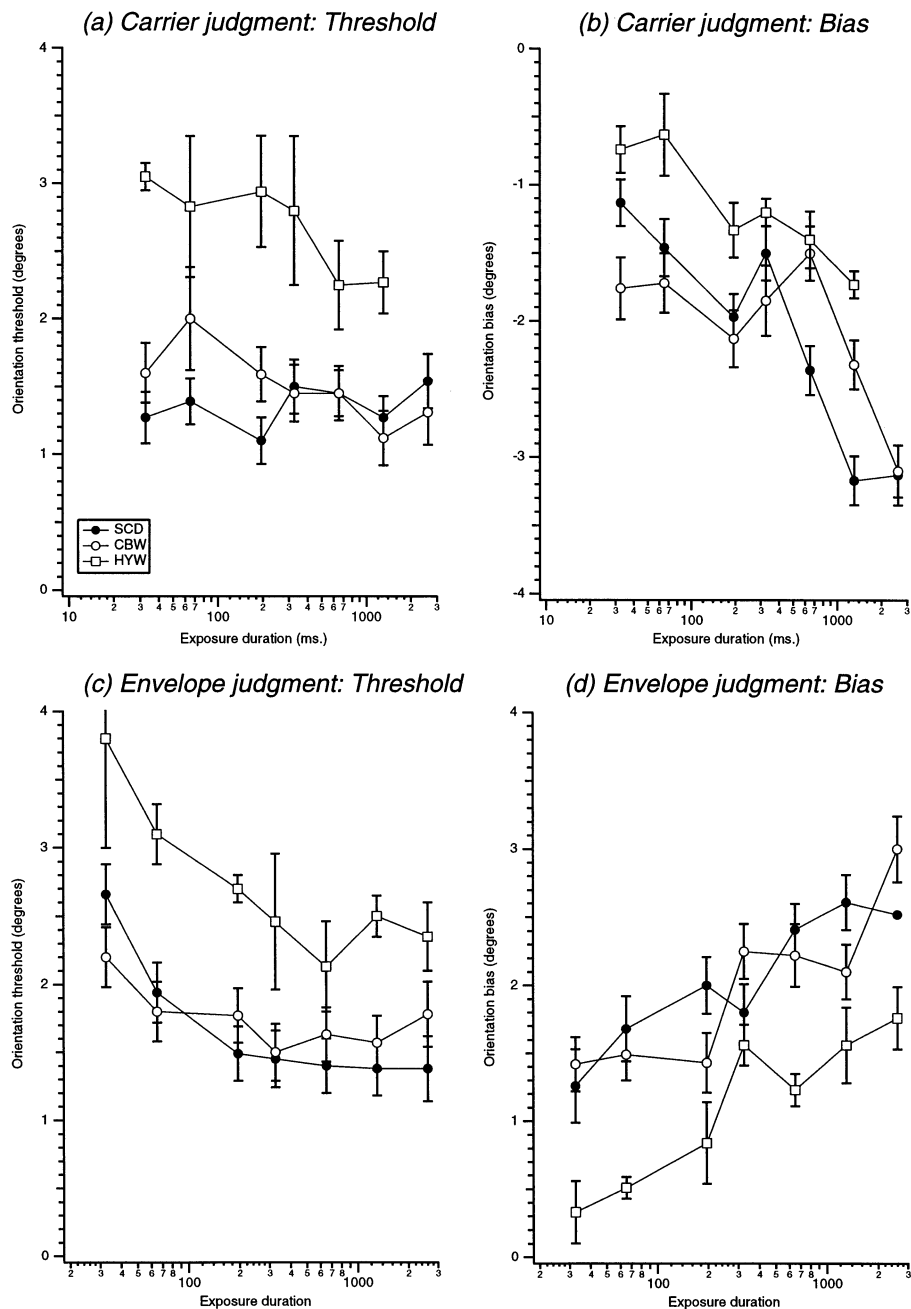


Fig. 10. Envelope and carrier orientation discrimination (upper and lower graphs, respectively) as a function of exposure duration. (a, c) show thresholds and (b, d) biases. Accuracy of second-order orientation judgements was much reduced for second-order compared to first-order patterns. Bias data indicates that the magnitude of illusory tilt of both envelope and carrier components of the Gabor, increase steadily with exposure duration.

### 6.1. Method

Stimuli were identical to those described above. All stimuli had a  $45^\circ$  orientation offset between carrier and envelope and had carriers fixed at 4 cpd. Given that stimuli were presented with a temporal Gaussian contrast window, the exposure time plotted is the period for which stimuli were presented at greater than 5% contrast (i.e.  $4.9 \sigma$ ).

### 6.2. Results

Fig. 10 shows data from the exposure duration condition. Accuracy of carrier orientation judgements was largely unaffected by exposure duration whereas accuracy of envelope discrimination is poor at short exposure times and plateaus at around 200 ms. These data are in good agreement with the experiments using D6 patterns described by Lin and Wilson (1996) and are

consistent with the suggestion therein that second-stage filtering requires more processing time. Interestingly, the bias data show that the illusory tilting of both carrier and envelope increases with prolonged exposure duration. Calvert and Harris (1988) similarly showed that the tilt illusion increases with exposure duration although they report a decrease beyond 100 ms which is not present in our data. Generally, our data indicate that the illusions we observe are not due to the second-order system operating under inappropriate conditions; the more time the second-order system is given to compute orientation the bigger the illusion gets. These illusions are therefore attributable to the organisation of the second-order system.

### 7. Modelling the effect of envelope orientation and carrier spatial frequency on judgement of carrier orientation

In this section we consider the effects of envelope orientation and carrier spatial frequency on carrier orientation judgements, in the context of a simple channel-coded model. This class of model operates on the output of linear spatial channels, assessing the energy across channels using some combination of these energy values to perform the psychophysical judgement. The work of Wilson and co-workers (for review see Wilson, 1991) have shown that channel-coded models are successful at explaining psychophysical performance on a variety of tasks involving orientation. This type of model achieves sub-channel resolution by means of

interpolation; i.e. they employ a distributed code for orientation. Changing the relative orientation of the envelope and the carrier will change the distribution of energy across channels, and in this section we examine if illusory shifts in carrier orientation could be attributable to this.

Fig. 11 illustrates the effect of changing the envelope orientation on the distribution of energy in the Fourier domain for stimuli from Experiment 2. Gabors with elongated envelopes are represented in the Fourier domain as two elliptical shaped regions of activity: the orientation of the line joining the centroids of these ellipses is the first-order orientation due to the carrier. The orientation of ellipses is the second-order orientation due to the envelope, which cannot be derived using a linear mechanism (which is symmetrical around the origin). The lower plots in the figure show energy as a function of orientation, pooled within the band indicated by the dashed region in the upper plots. Increasing the difference in orientation between carrier and envelope (i.e. going from a to c) increases the bandwidth activity across channels. Also, when carrier and envelope are non-parallel and non-perpendicular (Fig. 11b), the distribution of energy across orientation is asymmetrical. Consequently the peak energy across orientation remains fixed as the envelope rotates, but the mean orientation will change. Given that there is direct evidence that subject employ estimates of the local mean orientation to perform such tasks (e.g. Dakin & Watt, 1997) we sought to determine if the shift in the mean produced by such an asymmetry were sufficient to account for the illusory shift in perceived carrier

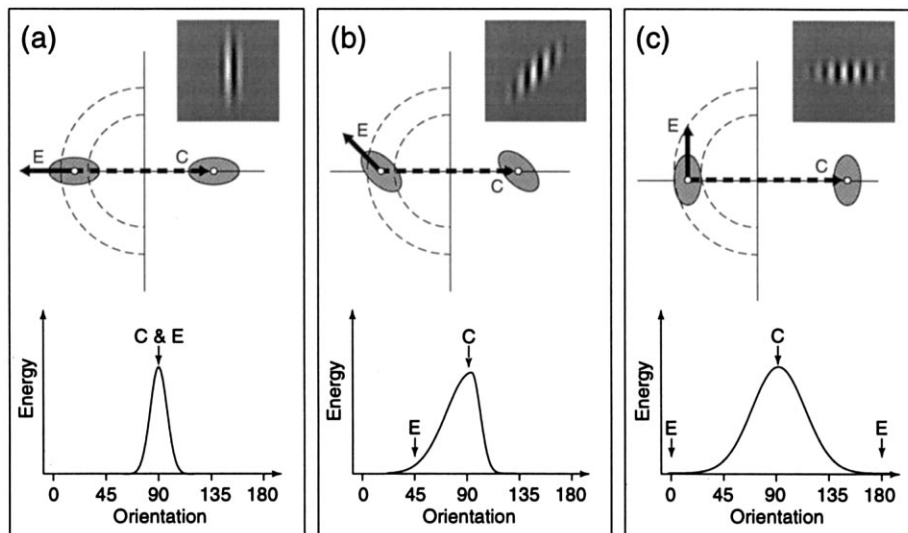


Fig. 11. The top graphs show schematic polar plots of Fourier energy for the inset stimuli, where the angle on the graph corresponds to orientation (rotated by 90° compared to orientation in the spatial domain), and the distance from the origin to spatial frequency. Gabors with elongated envelopes produce a pair of elliptical regions of high energy, where the ellipse orientation (solid arrow) corresponds to the envelope orientation and the orientation of line formed by joining the centroids of the two ellipses (dashed arrow) to the carrier orientation. The lower series of graphs are energy as a function of orientation within the interval indicated by the dashed region in upper plots. Notice the asymmetry in energy across orientation for the case when carrier and envelope are separated by 45° (shown in exaggerated form in the lower part of (b)).

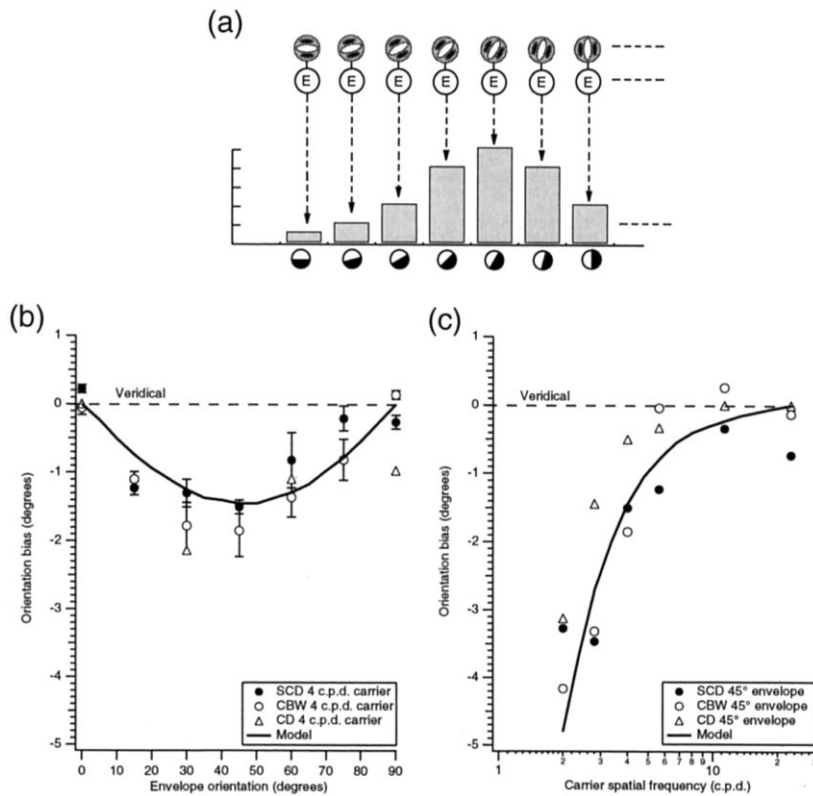


Fig. 12. (a) Cartoon of the first-order channel coded model. E refers to energy computation (squaring and summing across filtered image) An orientation estimate is derived by interpolating from a histogram of each filters energy. (b, c) Bias on carrier discrimination as a function of (b) envelope orientation and (c) carrier spatial frequency. Symbols show psychophysical data from Experiments 2 and 3, the solid lines are predictions from the channel coded model.

orientation measured in Experiment 2. In order to do this we formulated a simple channel-based model of orientation discrimination.

### 7.1. The channel-based model

An overview of the channel-coded model is presented in Fig. 12(a). The spatial filters used were D6 kernels (Wilson, 1991) defined by:

$$RF_i(x, y) = A_i \left[ \exp\left(\frac{-x^2}{\sigma_{1i}^2}\right) - B_i \exp\left(\frac{-x^2}{\sigma_{2i}^2}\right) + C_i \exp\left(\frac{-x^2}{\sigma_{3i}^2}\right) \right] \exp\left(\frac{-y^2}{\sigma_{yi}^2}\right) \quad (5)$$

where  $x$  and  $y$  are co-ordinates rotated by the filter orientation (using the standard equations). For a 4 cpd channel,  $A = 1.000$ ,  $B = 0.894$ ,  $C = 0.333$ ,  $\sigma_1 = 0.059^\circ$ ,  $\sigma_2 = 0.132^\circ$  and  $\sigma_3 = 0.177^\circ$ , and  $\sigma_y = 3.2 \sigma_1$ . This filter may be scaled and rotated accordingly to give sensitivity to various spatial frequencies and orientations. We used a filter bank composed of 12 orientations; from 0 to  $165^\circ$  in  $15^\circ$  steps, all at the optimal spatial frequency of the carrier.

In order to generate an orientation estimate from the model, the stimulus was convolved with the filter bank

and the output of each filter was squared and summed over the image, to give a measure of channel activity at each orientation. The final estimate of orientation was then computed as the mean of the channel orientation weighted by the activity of each channel (Dakin, 1997) although other methods for estimating the mean (e.g. parabolic interpolation between the three most active channels) produce similar predictions. For a bank of 12 filters each having an orientational bandwidth of around  $15^\circ$ , such interpolation techniques produce orientation thresholds of around  $1.5^\circ$  (in accord with psychophysical estimates of orientation discriminability for gratings).

### 7.2. Simulation procedure

The model was implemented in MatLab (Math Works Inc.) and an estimate of its bias was made using a method of bisection. For a fixed envelope orientation, the carrier orientation at which the model would signal vertical (the point of verticality) was bracketed between two orientations  $a$  and  $b$ , initially set to  $85^\circ$  and  $95^\circ$ , respectively. A Gabor stimulus was then generated with a carrier oriented at the mid-point  $(a + b)/2$  degrees and its orientation computed using the model. If the model

produced a bias clockwise of vertical, then  $a$  was set to the mid-point value otherwise  $b$  was set to this value. This procedure then iterated, with each iteration refining the bracketing of the predicted point of verticality until a stimulus was presented for which the model predicted zero bias. The offset of the carrier orientation at this point was recorded as the models' predicted bias.

This procedure was run as a function of both the envelope orientation (with carrier fixed at 4 cpd) and the carrier spatial frequency (with the envelope fixed at 45°) sampling these parameters twice as densely as in the psychophysical experiments reported above.

### 7.3. Results

The results of the simulation are compared to data from Experiments 2 and 3 in Fig. 12(b, c). Given the degree of variability of data that results from a judgement of the magnitude of an illusion, the model provides a reasonable account of the data. It would seem therefore that in order to account for the influence of the envelope on the perceived orientation of the carrier we do not need to make recourse to a specific combination mechanism. Instead the change in first order statistics produced by the rotating the envelope, when considered in the context of the likely early representation of orientation, is sufficient to account for the illusory tilt of the carrier observed.

## 8. Modelling the effect of carrier orientation and spatial frequency on judgement of envelope orientation

The results from Section 7 suggested that the influence of the envelope on perceived carrier orientation was explicable by the degree to which second-order structure affects the response of linear mechanisms, without the need to invoke the notion of explicit cue combination. However, subjects show the converse dependency of perceived envelope orientation on carrier orientation. This means that the visual module responsible for demodulating the second-order structure in our stimuli is far from ideal since it cannot ignore first-order structure. In this section we examine if these results are consistent with existing formulations of the filter-rectify-filter model described in Section 1.

### 8.1. The filter-rectify-filter model

The basic FRF model has two stages; a bank of linear D6 filters tuned to the peak spatial frequency of the stimuli, and a second bank operating on the rectified output of the first bank and tuned to a lower spatial frequency (Fig. 13a, b). The first variant on this model (Fig. 13a) has complete connectivity between a

bank of first- and second-stage filters. To determine a single estimate of envelope orientation the responses of second-stage filters are pooled across the preferred orientation of their first-stage filters. An estimate of mean orientation is then generated in a similar way to that described for the linear channel model. The second variant (the pooled first-stage model; Fig. 13b) sums the outputs of first-stage filters across orientation prior to filtering. This is equivalent to isotropic first-stage filtering. The final variant (the early non-linearity model) omits first-stage filters entirely and simply rectifies the stimulus prior to filtering.

Details of the simulation are similar to those described for the modelling of perceived carrier orientation, except that now the envelope orientation was varied to determine the zero-bias point of the models, for a range of different carrier orientations and carrier spatial frequencies.

### 8.2. Results

Predictions from the three models tested are presented in Fig. 13, along with psychophysical data from Experiments 2 and 3. Notice first that the early non-linearity predicts no illusory shifts; this model perfectly demodulates the envelope irrespective of the carrier orientation or spatial frequency. Human data are clearly not consistent with such a prediction. The second, and quite surprising finding of the simulation is that the completely connected FRF model performs poorly and produces large biases towards the carrier orientation which is, in most cases, in the opposite direction to the psychophysical data. This is due entirely to the oriented first-stage mechanisms distorting the shape of the envelope by highlighting orientation structure falling in their pass-band, which in turn biases the response of second-order filters towards the carrier orientation. Pooling across orientations prior to second-stage filtering reduces this problem and predicts a small repulsive influence of carrier on envelope. Overall, for both the spatial frequency and relative orientation conditions none of the models produce a good account of psychophysical data.

We varied a number of features of the model to attempt to get a better correspondence with psychophysical data. Various forms of early non-linearity (compressive, local gain control) produce similar (bias-free) predictions. Changing the form of the intermediate non-linearity from full-wave to half-wave rectification or to various power-law relationships has little effect on predictions. Mistuning of first-stage filters (as might be produced by having a series of second-stage mechanisms in a fixed spatial frequency relationship with first-stage mechanisms) increases the magnitude of the predicted illusion for the case of the summed first stage model but data are still substantially below subjects'

biases and show no reversal of the illusion in the relative orientation effect. Changing the first-stage combination rule from summation to a winner-take-all system across orientation (either channel-by-channel or locally, pixel-by-pixel) does not improve the quality of predictions. Reducing the aspect ratio of first-stage filters from 3.2:1 to 1:1 (therefore effectively increasing their orientational and spatial frequency bandwidth) drastically improves the precision of the fully connected FRF system, reducing bias to levels shown by the summed first-stage model. This finding is informative. It suggests that increasing the bandwidth of first-order mechanisms could assist in disambiguating whether second-stage filters respond to luminance or contrast-defined features.

To summarise: the illusory tilting of the Gabor envelope observed in Experiments 2 and 3 is not quantitatively explicable using a simple two-stage filter-rectify-filter version of the channel model described above.

### 9. Discussion

The key points of the paper are as follows:

- For Gabor patterns, a fixed carrier interferes with judgement of the envelope orientation. Subthreshold cues added to the carrier reduce this interference indicating that its site is early.

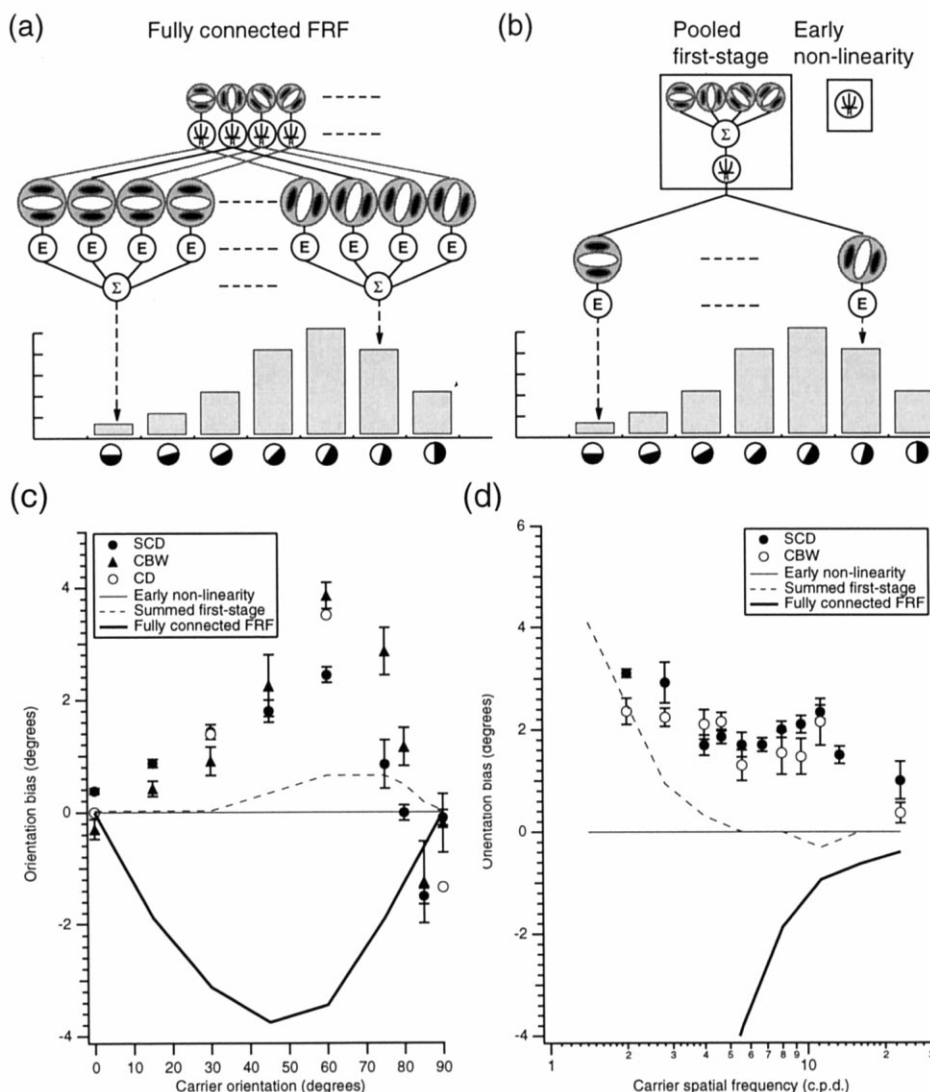


Fig. 13. (a, b) Cartoon of the E;RF channel coded models. E refers to energy computation (squaring and summing across filtered image) (a) Model 1 maintains independent connectivity between first- and second stage filters, with the latter being pooled to form a single second-order orientation channel. (b) Models 2 and 3 use variants on the first stage filters to reduce the amount of required connectivity. Model 2 has no first stage filters and uses an early rectifying non-linearity, and Model 3 uses isotropic first-stage filters built by summing the outputs of all first-stage filters. (c, d) Human data from Experiments 2 and 3 compared to predictions from the FRF channel models. Spatial frequency data are for the mid viewing distance.

- The orientation of the envelope has an attractive influence on the perceived orientation of the carrier. This is quantitatively consistent with a simple channel-based distributed code for first-order orientation.
- The orientation of the carrier has a repulsive influence on the perceived orientation of the envelope, until it is within 10° at which point the direction of the illusion reverses.
- This pattern of results is not consistent with existing filter-rectify-filter models of the coding of second-order structure.
- These orientation illusions increase with exposure duration and decreasing carrier spatial frequency.
- The precision and accuracy of envelope orientation discrimination is not scale invariant adding further weight to the argument that interference from the carrier is early.

### 9.1. Combination of first- and second-order orientation

The perceived orientation of the carrier component of our Gabor stimuli appears persistently tilted towards the envelope, when carrier and envelope were both non-parallel and non-perpendicular. Simulations using a simple channel based model demonstrated that this was likely to be due to the orientational skew on first-order orientation introduced by the envelope, and not to an active combination process between first- and second-order orientation cues. This is sensible from a functional point of view. If the visual system goes to the trouble of deriving two independent sources of information about local orientation, why should it rigidly combine them rather than maintain an independent representation of each?

The observed envelope illusion is not explicable in terms of a simple FRF model. Within the context of such a model, it seems that the envelope illusion is due either to the active combination of first- and second-stage cues to orientation, or to the selective connectivity of first- to second-stage filters. Data from Experiment 1 suggest that it is unlikely to be the former, since we demonstrated that the site of interference was low-level, presumably preceding second-stage filtering. It seems that the organisation of first-stage filters in relationship to the second-stage filters are responsible, and in the following section we speculate on what kind of organisation might lead to this pattern of results.

### 9.2. Linking contour integration and second-order processing?

Second-order structure is probably most usefully defined as anything which cannot be signalled directly by the output of a linear filter. Assuming that early visual processing can be usefully characterised as a predominantly linear system (as suggested by a sizeable

body of psychophysics), the essence of FRF is that output from linear filters can be *combined* into something useful by rectifying and re-filtering. Previously unassociated filters will be linked via the operation of a second-stage mechanism. What is the computational motivation for performing filter combination? The V1 representation is a mosaic of spatially localised band limited estimates of orientation and the spatial-frequency. There are a number of initial linking operations that are sensible first steps towards deriving complex image structure from this mosaic but one of the most fundamental is combination across orientation and space in order to make explicit the presence of *visual contours*. It is known that the local orientation is critical to supporting the detection of *visual contours* (Field, Hayes & Hess, 1993). Therefore, if second order filters are involved in contour integration we would expect that they would be subserved by first-order filters that are of the same or similar orientation as themselves. However, it is also known that we can detect, at a reduced level of performance, contours composed of elements *perpendicular* to the local contour direction (Field et al., 1993). This suggests that we have a second mechanism receiving inputs from first-stage filters oriented perpendicular to the contour direction. Our poor performance with these contours suggests that first-stage mechanisms may be more broadly tuned than for the former system. Fig. 14 illustrates these two contour integration systems, termed the contrast sensitive and insensitive contour integration systems, realised in terms of a filter-rectify-filter scheme. The important feature to notice here is that now the orientation of the second-stage filter is linked to the orientation of the first. The stage marked C denotes a combination stage. Our data indicate that combination (rather than say winner-take-all selection) does arise; that carrier orientations of 80° produce little illusory tilt of the envelope suggest that one system is playing off against the other. The form of this combination rule has yet to be determined.

The lower part of Fig. 14 illustrates how this type of model might explain the envelope illusion. The repulsive effects observed (middle histogram) are due to partial stimulation of adjacent second-stage filters receiving perpendicular first-stage inputs. Attraction effects (lower histogram) arise second-stage filters integrating parallel inputs are subserved by relatively narrowly tuned first-stage mechanisms, so that the response histogram is dominated by the response of the second-stage mechanism whose first-order input most closely matches the carrier.

This model remains speculative, but we suggest that it does have a number of advantages over the fully connected FRF model. First, it disambiguates whether input is derived from luminance or contrast define structure in the image avoiding the problems observed

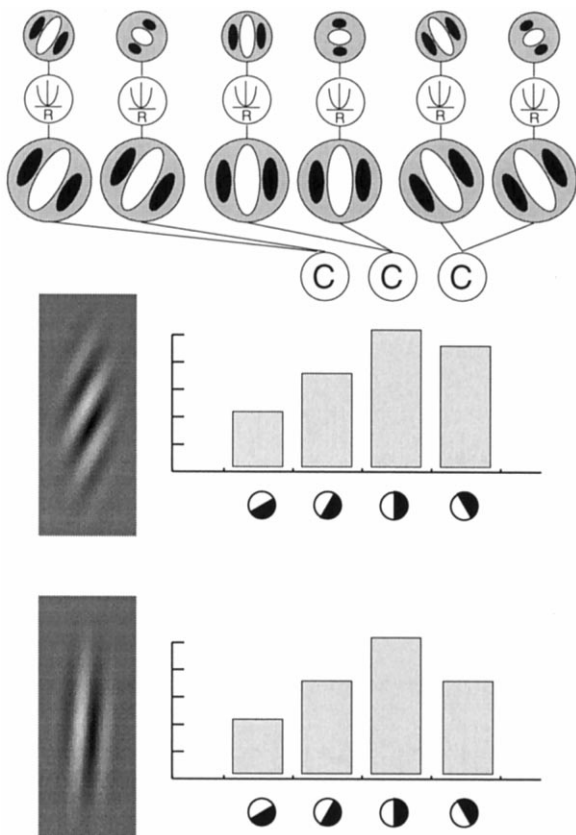


Fig. 14. An FRF model where second-stage filters receive inputs only from first-stage filters oriented parallel or perpendicular to their own orientation. The C stage indicates a combination stage whose form is as yet unknown. The first type of channel is a contrast-sensitive contour integrator, the second a contrast-insensitive contour integrator. The lower section of the figure illustrates how such a scheme could produce repulsion and attraction of envelope orientation to the carrier.

with the fully connected FRF system seen above. Second, the distinction it draws has functional significance in signalling if local contour is defined by luminance or contrast structure. Third, it avoids the proliferation of filters that are required for the fully connected FRF system.

### Acknowledgements

The authors are grateful to Isabelle Mareschal, Michael Morgan, and Hugh Wilson for providing many helpful comments on this project. This work was funded by a Canadian MRC grant (MT 108–18) to R.F. Hess.

### References

Badcock, D. R., & Derrington, A. M. (1989). Detecting the displacement of spatial beats: no role for distortion products. *Vision Research*, 29, 731–739.

- Burr, D. C., & Wijesundra, S. A. (1991). Orientation discrimination depends on spatial frequency. *Vision Research*, 31, 1449–1452.
- Calvert, J. E., & Harris, J. P. (1988). Spatial frequency and duration effects on the tilt illusion and orientation acuity. *Vision Research*, 28, 1051–1059.
- Chubb, C., & Sperling, G. (1988). Drift-balanced random stimuli: a general basis for studying non-Fourier motion perception. *Journal of the Optical Society of America A—Optics Image Science*, 5, 1986–2007.
- Cropper, S. J., & Badcock, D. R. (1995). Perceived direction of motion: it takes all orientations. *Perception*, 24, 106a.
- Dakin, S. C. (1997). The detection of structure in Glass patterns: psychophysics and computational models. *Vision Research*, 37, 2227–2259.
- Dakin, S. C., & Mareschal, I. Sensitivity to contrast modulation depends on carrier spatial frequency and orientation. *Vision Research*, (submitted).
- Dakin, S. C., & Watt, R. J. (1997). The computation of orientation statistics from visual texture. *Vision Research*, 37, 3181–3192.
- Derrington, A. M., & Badcock, D. R. (1986). Detection of spatial beats: non-linearity or contrast increment detection? *Vision Research*, 26, 343–348.
- Field, D. J., Hayes, A., & Hess, R. F. (1993). Contour integration by the human visual system: evidence for a local association field. *Vision Research*, 33, 173–193.
- Graham, N., Beck, J., & Sutter, A. (1992). Nonlinear processes in spatial-frequency channel models of perceived texture segregation: effects of sign and amount of contrast. *Vision Research*, 32, 719–743.
- Graham, N. V. S. (1989). *Visual pattern analyzers*. New York: Oxford University.
- Graham, N. V. S., & Nachmias, J. (1971). Detection of grating patterns containing two spatial frequencies. *Vision Research*, 11, 251–259.
- Heeley, D. W., & Buchanan-Smith, H. M. (1990). Recognition of stimulus orientation. *Vision Research*, 32, 719–743.
- Henning, G. B., Hertz, B. G., & Broadbent, D. E. (1975). Some experiments bearing on the hypothesis that the visual system analyses spatial frequency patterns in independent bands of spatial frequency. *Vision Research*, 15, 887–899.
- Hess, R. F., & Wilcox, L. M. (1994). Linear and non-linear filtering in stereopsis. *Vision Research*, 18, 2431–2438.
- Johnston, A., McOwan, P., & Buxton, H. (1992). A computational model of the analysis of some first-order and second-order motion patterns by simple and complex cells. *Proceedings of the Royal Society of London*, B250, 297–306.
- Kulikowski, J. J., & King-Smith, P. E. (1973). Spatial arrangement of line, edge, and grating detectors revealed by subthreshold summation. *Vision Research*, 13, 1455–1478.
- Lin, L., & Wilson, H. R. (1996). Fourier and non-Fourier pattern discrimination compared. *Vision Research*, 36, 1907–1918.
- Lu, Z. L., & Sperling, G. (1995). The functional architecture of human visual motion perception. *Vision Research*, 35, 2697–2722.
- Malik, J., & Perona, P. (1990). Preattentive texture discrimination with early visual mechanisms. *Journal of the Optical Society of America*, A7, 923–932.
- Mareschal, I., & Baker, C. L. (1998). A cortical locus for the processing of contrast defined visual stimuli. *Nature Neuroscience*, 1, 150–154.
- McOwan, P. W., & Johnson, A. (1995). A second-order pattern reveals separate strategies for encoding orientation in two-dimensional space and space-time. *Vision Research*, 36, 815425–815430.
- Morgan, M. J., & Baldassi, S. (1997). How the visual system encodes the orientation of a texture and why it makes mistakes. *Current Biology*, 7, 999–1002.
- Morgan, M. J., & Moulden, B. (1986). The Münsterberg figure and twisted cords. *Vision Research*, 26, 1793–1800.

- Münsterberg, H. (1897). Die verschobene Schachbrettfigur. *Z. Psychol.*, 5, 185–188.
- Pelli, D. G. (1997). The VideoToolbox software for visual psychophysics: transforming number into movies. *Spatial Vision*, 10, 437–442.
- Sutter, A., Sperling, G., & Chubb, C. (1995). Measuring the spatial frequency selectivity of second-order texture mechanisms. *Vision Research*, 35, 915–924.
- Tyler, C. W., & Nakayama, K. (1984). Size interactions in the perception of orientation. In L. Spillman, & B. R. Wootton, *Sensory experience, adaptation and perception: Festschrift for Ivo Kohler*. Hillsdale, NJ: Lawrence Erlbaum.
- Wilson, H. R. (1978). Quantitative characterization of two types of line-spread function near the fovea. *Vision Research*, 18, 971–981.
- Wilson, H. R. (1991). Psychophysical models of spatial vision and hyperacuity. In D. Regan, *Spatial vision*. New York, NY: MacMillan.
- Wilson, H. R., Ferrera, P., & Yo, C. (1992). A psychophysically motivated model for two dimensional motion perception. *Visual Neuroscience*, 9, 79–97.
- Wilson, H. R., & Kim, J. (1994). Perceived motion in the vector sum direction. *Visual Neuroscience*, 6, 1205–1220.
- Zhou, Y. X., & Baker, C. L., Jr. (1993). A processing stream in mammalian visual cortex neurons for non-Fourier responses. *Science*, 261, 98–101.
- Zhou, Y. X., & Baker, C. L., Jr. (1994). Envelope-responsive neurons in areas 17 and 18 of cat. *Journal of Neurophysiology*, 72, 2134–2150.
- Zhou, Y. X., & Baker, C. L., Jr. (1996). Spatial properties of envelope-responsive cells in area 17 and 18 neurons of the cat. *Journal of Neurophysiology*, 75, 1038–1050.
- Zöllner, F. (1862). Über eine neue Art anorthoskopischer Zerrbilder. *Poggendorffs Annalen*, 117, 477–484.